Journal of Neuro-Oncology
https://doi.org/10.1007/s11060-022-03946-4

CLINICAL STUDY

Predicting EGFR mutation status by a deep learning approach in patients with non-small cell lung cancer brain metastases

Oz Haim[1] · Shani Abramov[1] · Ben Shofty[1,5] · Claudia Fanizzi[2] · Francesco DiMeco[2] · Netanell Avisdris[3,4] · Zvi Ram[1] · Moran Artzi[4] · Rachel Grossman[1]

Received: 2 November 2021 / Accepted: 4 January 2022
© The Author(s), under exclusive licence to Springer Science+Business Media, LLC, part of Springer Nature 2022

Abstract

Purpose Non-small cell lung cancer (NSCLC) tends to metastasize to the brain. Between 10 and 60% of NSCLCs harbor an activating mutation in the epidermal growth-factor receptor (EGFR), which may be targeted with selective EGFR inhibitors. However, due to a high discordance rate between the molecular profile of the primary tumor and the brain metastases (BMs), identifying an individual patient's EGFR status of the BMs necessitates tissue diagnosis via an invasive surgical procedure. We employed a deep learning (DL) method with the aim of noninvasive detection of the EGFR mutation status in NSCLC BM.

Methods We retrospectively collected clinical, radiological, and pathological-molecular data of all the NSCLC patients who had been diagnosed with BMs and underwent resection of their BM during 2009–2019. The study population was then divided into two groups based upon EGFR mutational status. We further employed a DL technique to classify the two groups according to their preoperative magnetic resonance imaging features. Augmentation techniques, transfer learning approach, and post-processing of the predicted results were applied to overcome the relatively small cohort. Finally, we established the accuracy of our model in predicting EGFR mutation status of BM of NSCLC.

Results Fifty-nine patients were included in the study, 16 patients harbored EGFR mutations. Our model predicted mutational status with mean accuracy of 89.8%, sensitivity of 68.7%, specificity of 97.7%, and a receiver operating characteristic curve value of 0.91 across the 5 validation datasets.

Conclusion DL-based noninvasive molecular characterization is feasible, has high accuracy and should be further validated in large prospective cohorts.

Keywords NSCLC · Brain · Metastasis · EGFR · MRI · Deep learning

Introduction

Lung cancer is the most commonly diagnosed type of cancer and the leading cause for cancer-associated mortality worldwide, with an incidence of 2.1 million new cases each year [1]. Non-small cell lung cancer (NSCLC) is the most prevalent among the lung cancer subtypes, accounting for about 85% of cases [2]. Brain metastases (BMs) are the most common intracranial neoplasm, and lung cancer is their main source [3]. Between 10 and 50% of NSCLC metastasize to the brain, depending upon characteristics of the primary tumor such as stage, molecular profile, and previous oncological treatments [4, 5]. Historically, patients with BMs were considered to have a very poor prognosis, with a median survival rate of 1–3 months [6]. Recent progress

✉ Rachel Grossman
rachelgr@tlvmc.gov.il

1 Department of Neurosurgery, Tel Aviv Medical Center, Affiliated to the Sackler Faculty of Medicine, Tel-Aviv University, 6 Weizman Street, 6423906 Tel-Aviv, Israel

2 Department of Neurosurgery, Fondazione IRCCS Istituto Neurologico C. Besta, Milan, Italy

3 School of Computer Science and Engineering, Hebrew University of Jerusalem, Jerusalem, Israel

4 Sagol Brain Institute, Tel Aviv Medical Center, and the Sackler Faculty of Medicine and Sagol School of Neuroscience, Tel Aviv University, Tel-Aviv, Israel

5 Department of Neurosurgery, Baylor College of Medicine, Houston, TX, USA

Published online: 04 February 2022

in this field has led to much improvement in survival in selected cases amenable to the new generation therapies [6].

Many genetic alterations have been found in NSCLC tumors, and the most fundamental driver mutations among them is the activation of mutations of the epidermal growth factor receptor (EGFR). EGFRs are proteins located on the cell membrane, and their endpoint is cell proliferation, which is activated in part by a cascade of tyrosine kinase signaling [7]. Activating mutations of EGFR are observed between 10 and 60% of NSCLC patients, affected among others by geographic and ethnic group [8]. Targeted therapy against EGFR, a subset of tyrosine kinase inhibitors (TKI) has recently replaced standard chemotherapy as first-line treatment in advanced metastatic NSCLC with improved response rates [9–11], even among the subgroup of patients with BMs [12]. Unfortunately, resistance to EGFR TKIs is not uncommon, as manifested in some cases by restoration of a wild-type EGFR profile [13]. Moreover, there is 30–55% of discordance between the molecular profile of the primary tumor and it's BMs, thus making it impossible to extrapolate the EGFR status of the BMs from the original tumor source [14–16].

Although knowing the EGFR status of each BM is crucial for treatment planning, it had been possible only via the information derived from a tumor specimen. Tailoring specific treatments for different mutations of NSCLC and diagnose changes in their molecular profile by radiological tools, may preclude the need for invasive procedures.

In recent years there has been significant progress in the use of artificial intelligence methods in the form of conventional machine learning [17] and deep learning (DL) for medical image analysis [18]. Indeed DL methodologies have become the state-of-the-art approach in various computer imaging capabilities, with extensive applications in medical image analysis [19–21]. Several studies have investigated the feasibility of conventional machine learning methods for the differentiation of NSCLC molecular subtypes, 2 of which targeted BM and used a radiomics approach [22, 23]. While radiomics has been suggested to have a real clinical impact in lung cancer [24], it also harbors some structured limitations [25, 26].

To the best of our knowledge, there has not been any analysis in which DL tools were assigned to delineate EGFR status in of BM in NSCLC patients. We therefore designed this work to apply DL analysis for this purpose.

Methods

Study design

This experimental, analytic, comparative study aimed at assessing the reliability of a noninvasive tool for classifying BMs from an NSCLC source according to their EGFR status. Data were collected retrospectively from the medical files of the study population. Pathological data based on histology were extracted from pathological reports following tissue biopsy, and EGFR status, as part of the clinical process, was determined by reverse transcription polymerase chain reaction.

Study population

We retrospectively collected the records of all NSCLC patients with BMs who underwent resection of their BMs in 2 institutions, Tel-Aviv Medical Center, Tel-Aviv, Israel between 2009 and 2019 (46 patients), and Fondazione IRCCS Istituto Neurologico C. Besta, Milan, Italy (13 patients). The patients were divided into two groups based upon their EGFR status of being positive or negative for EGFR mutation.

Included were all diagnosed NSCLC patients with BMs who were treatment naive, underwent resection of their BMs and for whom a histology-based pathological report, the molecular-based EGFR status, and a preoperative magnetic resonance imaging (MRI) study of sufficient quality were available. Our analysis was restricted to specific metastases which had been resected and for which their EGFR status had been determined. Preoperative MRI scans with major artifacts or of low quality, and scans of patients who had undergone radiation treatment to their BMs prior to the MRI were excluded. The study was approved by the local institutional review boards (IRB) in both centers, Tel-Aviv Medical Center, and Fondazio ne IRCCS Istituto Neurologico C. Besta, (IRB approval numbers 0200-10, and 81/2021, respectively).

Image analysis

Preprocessing

Analysis was performed on the post contrast T1 weighted MRI images (T1W + c), and included bias field correction with an intensity inhomogeneity correction algorithm (SPM, part of MATLAB R2019b) [27], and intensity normalization by the equation: $normalize(x) = \frac{xi-\bar{x}}{(\sigma)}$ where xi is the value of given voxel in the image, $\bar{x}$ *and* σ are the mean and standard deviation of the brain extracted image. Tumor segmentation was performed by senior neurosurgeon and using commercial software (AnalyzeDirect 11.0) at the slice (2D) level. For each patient only one lesion was extracted (the resected metastasis). The extracted mask was then used to generate crop images (i.e., delimitation of the lesion mask and its surrounding).

Data splitting

The entire dataset was split at the subject level into 80% training (236 samples) and 20% validation (57 samples) datasets in a stratified fivefold cross-validation manner proportional to group size, and ensuring that all images belonging to a given patient would be allocated to the same group.

DL analysis

DL model training and evaluation were performed by means of the Fast.ai framework built on top of the PyTorch environment [28].

The input data for the DL analysis were cropped images of the mid-tumor region and ± 2 slices (total of 5 slices), all extracted from the normalized T1W + c image and resized to a 96 × 96 image size (Fig. 1). All extracted samples were manually reviewed in order to ensure proper image quality and no partial volume artifact. Data augmentation was performed in order to increase the dataset size and variance, and it included random rotations, zooming, and contrast modification. In addition, mixup augmentation [29] was applied for combining training samples by means of their linear combinations.

A ResNet-50 [30] convolutional neural network was set as the network's architecture. Network training was carried out by means of F1 loss function with an initial learning rate of $4e^{-2}$ and a batch size of 32. The metric for evaluating the model during training was the F1 score. Data oversampling was employed in order to cope with the imbalanced datasets, enabling sampling of the two groups in roughly equal amounts.

Due to the relatively small data size that was available for this study a transfer learning was performed, the network was trained using a pre-trained ResNet-50 model, trained on an ImageNet data set as previously described in detail elsewhere [31, 32]. Training was performed with a total of 40 epochs while preserving the model which achieved the best level of accuracy during the process.

Post-processing of the predicted results was performed at the subject level by calculation of a predication score for the adjacent slices and tested based upon median, maximum, minimum, and mean metrics (Fig. 1).

The classification results were evaluated on the validation datasets, for each one of the fivefolds, using accuracy, precision, recall, F1 score and receiver- operating characteristic curve (ROC).

Results

Patient characteristics

Preoperative post-contrast T1-weighted images (T1WI + c) of 59 patients with NSCLC BMs were reviewed. Forty-three of those patients (62 ± 12 years old, 15 females) had a negative EGFR mutational status and 16 patients (62 ± 11 years old, 11 females) had a positive EGFR mutational status. The study patients' characteristics are summarized in Table 1. There were no significant differences between the positive and negative status groups except for female dominance in the EGFR mutant group and male dominance in EGFR wild-type group, t = 2.403, p = 0.02).

Classification results

The fivefold cross validation results are presented in Table 2. The best classification results were obtained by using the median metric for the post-processing of the predicted results, with an overall accuracy of 89.8%, a sensitivity of 68.7%, and a specificity of 97.7% for the detection of a positive EGFR mutation status. The mean and median metrics

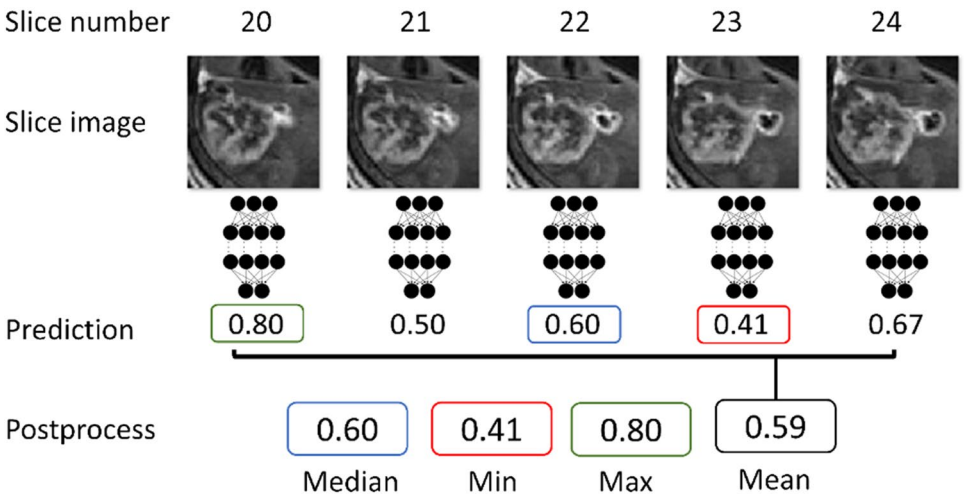

Fig. 1 Post-processing phase. The numbers for each slice indicating the predicted model EGFR score. Each post-processing metric was calculated based upon the 5-slice context scores

Table 1 Clinical characteristics of NSCLC patients with BMs who underwent resection of their BMs

Characteristics	EGFR wild type (N = 43)		EGFR mutant (N = 16)		P-value	
Age (years, Median ± SD)	61.81)11.82(		62.13)10.65(		0.709	
Sex						
Male	28 (65%)		5 (31%)		*0.02*	
Female	15 (35%)		11 (69%)		*0.02*	
Location (involved lobe)	Lt	Rt	Lt	Rt	Lt	Rt
Frontal	20.4%	26.06%	24.75%	20.96%	0.680	0.658
Parietal	5.79%	1.35%	4.52%	9.77%	0.815	0.114
Temporal	6.79%	0.57%	1.11%	3.35%	0.230	0.188
Occipital	1.16%	2.09%	0.26%	0.12%	0.566	0.570
Limbic	5.55%	2.05%	0.48%	2.01%	0.076	0.983
Subcortical	6.58%	7.06%	6.43%	1.30%	0.977	0.244
Cerebellar	2.41%	11.75%	5.94%	19.01%	0.486	0.475
Brainstem	0.17%	0.22%	0%	0%	0.523	0.507
Tumor Volume (cm^3, Mean ± SD)						
T1WI + c	1.21)0.58(		0.96)0.52(		0.125	

Data are median (SD) or number (%)

EGFR epidermal growth factor receptor

Table 2 Fivefold cross validation results for the different post-processing metrics

Fold	Cross validation ROC					Overall ROC		At network result threshold 0.5		
	1	2	3	4	5	Mean	SD	Sensitivity (%)	Specificity (%)	Accuracy (%)
Min	0.84	0.93	0.93	**0.92**	**0.81**	0.88	0.05	62.5	97.7	88.1
Max	0.91	**1.00**	**1.00**	0.67	0.78	0.87	0.13	62.5	97.7	88.1
Median	0.88	**1.00**	0.96	**0.92**	**0.81**	**0.91**	**0.07**	**68.7**	**97.7**	**89.8**
Mean	**0.94**	**1.00**	**1.00**	0.83	0.78	**0.91**	0.09	**68.7**	**97.7**	**89.8**

Bolded are top results

ROC receiver operating characteristic curve

achieved similar results of a mean ROC of 0.91, while the variability was lower for the median metric (0.07) compared to the mean metric (0.09), indicating the stability of the median metric. While the specificity of all post-processing methods was same (97.7%), both best performing methods (median and mean) achieved better sensitivity (68.7%), indicating that some slices were more informative than others in the EGFR mutation status prediction task. Figure 2 shows an ROC curve for the classification for the best performing post-processing metric (median) between the positive and negative EGFR mutations. The mean ROC value across the 5 validation datasets was 0.91 ± 0.07 (Fig. 2).

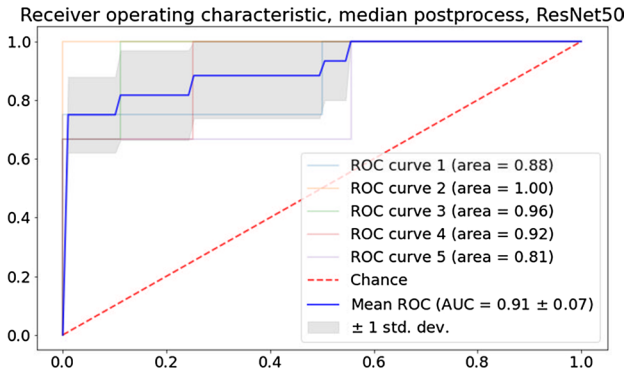

Fig. 2 Receiver operating characteristic, median slice metric, fivefold combined. *ROC* receiver operating characteristic curve, *ResNet* residual neural network

Discussion

This study provides a proof of concept that DL analysis can be applied for the prediction of EGFR mutation status in NSCLC BMs. The study is based on a relatively small cohort (n = 59). We addressed this challenge by using the several techniques including training the model based on the slice level (2D) and extracting ~ 5 slices from each patient followed by post-processing of the predicted results at the patient level, applying extensive augmentation techniques including random rotations, zooming, contrast modification and mix-up augmentation, and using transfer learning training approach, shown to be preferable for small cohorts comparing to training from scratch [33–35]. By extracting data from a limited number of patients (n = 59), applying the above-described augmentation technics and the transfer learning approach, together with post-processing of the predicted results, we were able to classify the patients according to their EGFR mutation status. This allowed us to reach an overall accuracy of 89.8%, a sensitivity of 68.7%, and a specificity of 97.7% for the detection of a positive EGFR mutation status.

Looking forward, one should expect machine learning technologies to become an inseparable part of our diagnostic workup and decision-making process. Chest computerized tomographic (CT)-based radiomics analysis was established as a ground-breaking tool for discriminating between different molecular subtypes of NSCLC (including EGFR, ALK and KRAS mutations) [36]. Oikonomou et al. used positron emission tomography-CT-based radiomics to predict response to stereotactic body radiotherapy in lung cancer patients. Those authors found radiomics as being the only predictor for local control [37]. Hosny et al. investigated the predictive value of DL for mortality risk stratification in NSCLC. They incorporated several datasets to build a database of 1200 patients, and applied convolutional neural networks based upon an analysis of CT scans to predict the response to radiation therapy and surgery. They reported area under the curve (AUC) values of 0.70 and 0.71, respectively, and succeeded in stratifying patients into low and high mortality risk following both radiotherapy ($p < 0.001$) and surgery ($p = 0.03$) using the same tool [38]. Trebeschi et al. showed that standard-of-care imaging may serve as a base for machine learning to predict response to immunotherapy in NSCLC and melanoma patients. Their radiomics-based prediction tool for anti PD-L1 response achieved an AUC up to 0.83 for patients with NSCLC, with a survival advantage of 25% at 1 year following treatment [39].

It is highly significant to have the ability to combine a comprehensive molecular profile of each involved site while minimizing the invasiveness of the diagnostic workup and providing tailored treatment in the setting of BMs. Ramón et al. used MRI-based radiomics tools to differentiate lung origin of BMs from breast and melanoma origins with an accuracy of 90% [40].

Two trials were recently conducted in the field of machine learning for the prediction of EGFR status in NSCLC BM. Ahn et al. applied MRI based radiomics on 210 metastases (61 patients, of whom 29 were EGFR positive according to their lung pathology findings) and reached a diagnostic accuracy of 86.7% (AUC 0.868) [22]. Park et al. reached a diagnostic accuracy and an AUC of 78.6% and 0.73, respectively, utilizing radiomics tools based upon MRI features of 99 BMs (51 patients, of whom 42 were EGFR positive as confirmed by biopsy of at least one of the BMs) [23]. While trying to demonstrate a proof of concept for radiomics prediction of EGFR status in NSCLC BMs, both of these trials assumed an identical molecular profile between the sampled tissue and the rest of the metastases, an assumption that has since been shown to be not necessarily accurate [13–15]. Moreover, radiomics analysis is based upon a handcrafted image processing pipeline which includes feature extraction, feature selection, and machine learning model building. Any small change in any one of these steps may impair its prediction accuracy and stability.

Our results demonstrated a promising potential of utilizing a DL approach based on standard clinical MRI for noninvasive assessment of EGFR mutation status in BM of NSCLC patients. Although less accurate than histology-based results, it might be useful for treating patients who are not suitable for surgery and for those with eloquent-seated lesions or poly-metastatic disease. Notably, although our study provides proof of concept for DL based prediction of EGFR status in BM originated from NSCLC, further research with a larger dataset, composed of additional MRI sequences from varied populations and institutions, is required to validate our results with the aim of developing a robust and reliable computer aided diagnostic tool with high rate of generalizability.

Study limitations

The main limitation of this study derives from the relatively small number of patients. Our sample size stems partly from the stringent study inclusion criteria and the current trend to radiate upfront many of those patients without pathological diagnosis. This limitation apparently represents a real-world challenge when attempting to conclusively verify the utility of DL for predicting EGFR mutation status in patients with BM from lung cancer.

Conclusions

Determining the molecular profile of NSCLC BMs non-invasively is feasible with standard imaging studies by applying a DL tool. This technology has the potential to improve the personalized treatment paradigm of these patients. Despite being trained on a small cohort of patients, our classifier accurately predicted EGFR mutations when compare to previous works. Further research based on larger cohorts from different centers in diverse communities is warranted in order to create a reliable tool for widespread clinical use.

Author contributions OH, BS, ZR, MA and RG contributed to the study conception and design. Material preparation and data collection were performed by SA, OH and CF, analysis was performed by MA and NA. The first draft of the manuscript was written by OH and all authors commented on previous versions of the manuscript. All authors read and approved the final manuscript.

Funding This research did not receive any specific grant from funding agencies in the public, commercial, or not-for-profit sectors.

Data availability All the data in this study is available in Sagol Brain Institute, Tel Aviv Medical Center, Tel-Aviv, Israel.

Code availability Not applicable.

Declarations

Conflict of interest The authors declare no competing interests.

Ethical approval Tel-Aviv Medical Center, and Fondazio ne IRCCS Istituto Neurologico C. Besta, (IRB approval numbers 0200-10, and 81/2021, respectively).

Consent to participate Not applicable.

Consent for publication Not applicable.

References

1. Bray F, Ferlay J, Soerjomataram I et al (2018) Global cancer statistics 2018: GLOBOCAN estimates of incidence and mortality worldwide for 36 cancers in 185 countries. CA Cancer J Clin 68:394–424. https://doi.org/10.3322/caac.21492
2. Molina JR, Yang P, Cassivi SD et al (2008) Non-small cell lung cancer: epidemiology, risk factors, treatment, and survivorship. Mayo Clin Proc 83:584–594. https://doi.org/10.4065/83.5.584
3. Schouten LJ, Rutten J, Huveneers HAM, Twijnstra A (2002) Incidence of brain metastases in a cohort of patients with carcinoma of the breast, colon, kidney, and lung and melanoma. Cancer 94:2698–2705. https://doi.org/10.1002/cncr.10541
4. Chi A, Komaki R (2010) Treatment of brain metastasis from lung cancer. Cancers 2:2100–2137. https://doi.org/10.3390/cancers2042100
5. Shin D-Y, Na II, Kim CH et al (2014) EGFR mutation and brain metastasis in pulmonary adenocarcinomas. J Thorac Oncol 9:195–199. https://doi.org/10.1097/JTO.0000000000000069
6. Ali A, Goffin JR, Arnold A, Ellis PM (2013) Survival of patients with non-small-cell lung cancer after a diagnosis of brain metastases. Curr Oncol Tor Ont 20:e300-306. https://doi.org/10.3747/co.20.1481
7. Oda K, Matsuoka Y, Funahashi A, Kitano H (2005) A comprehensive pathway map of epidermal growth factor receptor signaling. Mol Syst Biol 1:E1–E17. https://doi.org/10.1038/msb4100014
8. Midha A, Dearden S, McCormack R (2015) EGFR mutation incidence in non-small-cell lung cancer of adenocarcinoma histology: a systematic review and global map by ethnicity (mutMapII). Am J Cancer Res 5:2892–2911
9. Mok TS, Wu Y-L, Thongprasert S et al (2009) Gefitinib or carboplatin–paclitaxel in pulmonary adenocarcinoma. N Engl J Med 361:947–957. https://doi.org/10.1056/NEJMoa0810699
10. Rosell R, Carcereny E, Gervais R et al (2012) Erlotinib versus standard chemotherapy as first-line treatment for European patients with advanced EGFR mutation-positive non-small-cell lung cancer (EURTAC): a multicentre, open-label, randomised phase 3 trial. Lancet Oncol 13:239–246. https://doi.org/10.1016/S1470-2045(11)70393-X
11. Sequist LV, Yang JC-H, Yamamoto N et al (2013) Phase III study of afatinib or cisplatin plus pemetrexed in patients with metastatic lung adenocarcinoma with *EGFR* mutations. J Clin Oncol 31:3327–3334. https://doi.org/10.1200/JCO.2012.44.2806
12. Soria J-C, Ohe Y, Vansteenkiste J et al (2018) Osimertinib in untreated EGFR-mutated advanced non-small-cell lung cancer. N Engl J Med 378:113–125. https://doi.org/10.1056/NEJMoa1713137
13. Kalikaki A, Koutsopoulos A, Trypaki M et al (2008) Comparison of *EGFR* and *K-RAS* gene status between primary tumours and corresponding metastases in NSCLC. Br J Cancer 99:923. https://doi.org/10.1038/sj.bjc.6604629
14. Bozzetti C, Tiseo M, Lagrasta C et al (2008) Comparison between epidermal growth factor receptor (EGFR) gene expression in primary non-small cell lung cancer (NSCLC) and in fine-needle aspirates from distant metastatic sites. J Thorac Oncol 3:18–22. https://doi.org/10.1097/JTO.0b013e31815e8ba2
15. Brastianos PK, Carter SL, Santagata S et al (2015) Genomic characterization of brain metastases reveals branched evolution and potential therapeutic targets. Cancer Discov 5:1164–1177. https://doi.org/10.1158/2159-8290.CD-15-0369
16. Berger LA, Riesenberg H, Bokemeyer C, Atanackovic D (2013) CNS metastases in non-small-cell lung cancer: current role of EGFR-TKI therapy and future perspectives. Lung Cancer 80:242–248. https://doi.org/10.1016/j.lungcan.2013.02.004
17. Shofty B, Artzi M, Shtrozberg S et al (2020) Virtual biopsy using MRI radiomics for prediction of BRAF status in melanoma brain metastasis. Sci Rep 10:6623. https://doi.org/10.1038/s41598-020-63821-y
18. Quon JL, Bala W, Chen LC et al (2020) Deep learning for pediatric posterior fossa tumor detection and classification: a multi-institutional study. Am J Neuroradiol 41:1718–1725. https://doi.org/10.3174/ajnr.A6704
19. Lundervold AS, Lundervold A (2019) An overview of deep learning in medical imaging focusing on MRI. Z Für Med Phys 29:102–127. https://doi.org/10.1016/j.zemedi.2018.11.002
20. Litjens G, Kooi T, Bejnordi BE et al (2017) A survey on deep learning in medical image analysis. Med Image Anal 42:60–88. https://doi.org/10.1016/j.media.2017.07.005
21. Grossman R, Haim O, Abramov S et al (2021) Differentiating small-cell lung cancer from non-small-cell lung cancer brain metastases based on MRI using efficientnet and transfer learning

approach. Technol Cancer Res Treat 20:15330338211004920. https://doi.org/10.1177/15330338211004919
22. Ahn SJ, Kwon H, Yang J-J et al (2020) Contrast-enhanced T1-weighted image radiomics of brain metastases may predict EGFR mutation status in primary lung cancer. Sci Rep. https://doi.org/10.1038/s41598-020-65470-7
23. Park YW, An C, Lee J et al (2021) Diffusion tensor and postcontrast T1-weighted imaging radiomics to differentiate the epidermal growth factor receptor mutation status of brain metastases from non-small cell lung cancer. Neuroradiology 63:343–352. https://doi.org/10.1007/s00234-020-02529-2
24. Scrivener M, de Jong EEC, van Timmeren JE et al (2016) Radiomics applied to lung cancer: a review. Transl Cancer Res. https://doi.org/10.21037/8536
25. Li Q, Bai H, Chen Y et al (2017) A fully-automatic multiparametric radiomics model: towards reproducible and prognostic imaging signature for prediction of overall survival in glioblastoma multiforme. Sci Rep 7:14331. https://doi.org/10.1038/s41598-017-14753-7
26. Sun Q, Lin X, Zhao Y et al (2020) Deep learning vs. radiomics for predicting axillary lymph node metastasis of breast cancer using ultrasound images: don't forget the peritumoral region. Front Oncol. https://doi.org/10.3389/fonc.2020.00053
27. Ashburner J, Friston KJ (2005) Unified segmentation. Neuroimage 26:839–851. https://doi.org/10.1016/j.neuroimage.2005.02.018
28. Howard J, Gugger S (2020) Fastai: a layered API for deep learning. Information 11:108. https://doi.org/10.3390/info11020108
29. Zhang H, Cisse M, Dauphin YN, Lopez-Paz D (2018) mixup: beyond empirical risk minimization. ArXiv171009412 Cs Stat
30. Liu W, Anguelov D, Erhan D et al (2016) SSD: Single shot multibox detector. In: Leibe B, Matas J, Sebe N, Welling M (eds) Computer vision – ECCV 2016. Springer International Publishing, Cham, pp 21–37
31. Iglovikov V, Shvets A (2018) TernausNet: U-Net with VGG11 encoder pre-trained on imagenet for image segmentation. ArXiv180105746 Cs
32. Lau SLH, Chong EKP, Yang X, Wang X (2020) Automated pavement crack segmentation using U-Net-based convolutional neural network. IEEE Access 8:114892–114899. https://doi.org/10.1109/ACCESS.2020.3003638
33. Tajbakhsh N, Shin JY, Gurudu SR et al (2016) Convolutional neural networks for medical image analysis: full training or fine tuning? IEEE Trans Med Imaging 35:1299–1312. https://doi.org/10.1109/TMI.2016.2535302
34. Raghu M, Zhang C, Kleinberg J, Bengio S (2019) Transfusion: understanding transfer learning for medical imaging. In: Thrun S, Saul LK, Schölkopf B (eds) Advances in neural information processing systems. Curran Associates Inc, Red Hook
35. Frid-Adar M, Ben-Cohen A, Amer R, Greenspan H (2018) Improving the Segmentation of anatomical structures in chest radiographs using U-Net with an Imagenet pre-trained encoder. In: Third International Workshop, RAMBO 2018, Fourth International Workshop, BIA 2018, and First International Workshop, TIA 2018, Held in Conjunction with MICCAI 2018, Granada, Spain, September 16 and 20, 2018, Proceedings. pp 159–168
36. Chen B, Zhang R, Gan Y et al (2017) Development and clinical application of radiomics in lung cancer. Radiat Oncol 12:154. https://doi.org/10.1186/s13014-017-0885-x
37. Oikonomou A, Khalvati F, Tyrrell PN et al (2018) Radiomics analysis at PET/CT contributes to prognosis of recurrence and survival in lung cancer treated with stereotactic body radiotherapy. Sci Rep 8:4003. https://doi.org/10.1038/s41598-018-22357-y
38. Hosny A, Parmar C, Coroller TP et al (2018) Deep learning for lung cancer prognostication: a retrospective multi-cohort radiomics study. PLoS Med 15:e1002711. https://doi.org/10.1371/journal.pmed.1002711
39. Trebeschi S, Drago SG, Birkbak NJ et al (2019) Predicting response to cancer immunotherapy using noninvasive radiomic biomarkers. Ann Oncol Off J Eur Soc Med Oncol 30:998–1004. https://doi.org/10.1093/annonc/mdz108
40. Ortiz-Ramón R, Larroza A, Ruiz-España S et al (2018) Classifying brain metastases by their primary site of origin using a radiomics approach based on texture analysis: a feasibility study. Eur Radiol. https://doi.org/10.1007/s00330-018-5463-6

Publisher's Note Springer Nature remains neutral with regard to jurisdictional claims in published maps and institutional affiliations.